







PERSPECTIVE | MARCH 03 2021

The physics of plasma membrane photostimulation

Special Collection: [Advances in Bioelectronics: Materials, Devices, and Translational Applications](#)

Giovanni Manfredi ; Francesco Lodola ; Giuseppe Maria Paternó ; Vito Vurro; Pietro Baldelli ; Fabio Benfenati ; Guglielmo Lanzani 



APL Mater. 9, 030901 (2021)

<https://doi.org/10.1063/5.0037109>



View
Online

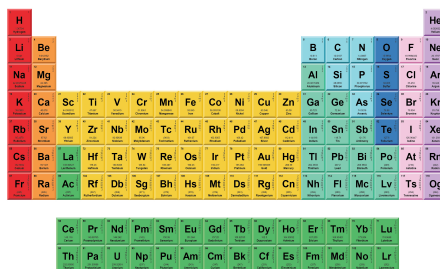


Export
Citation



THE MATERIALS SCIENCE MANUFACTURER®

Now Invent.™



American Elements
Opens a World of Possibilities

...Now Invent!

www.americanelements.com

© 2021-2024 American Elements LLC. All Rights Reserved. Trademark.

The physics of plasma membrane photostimulation

Cite as: *APL Mater.* 9, 030901 (2021); doi: [10.1063/5.0037109](https://doi.org/10.1063/5.0037109)
Submitted: 10 November 2020 • Accepted: 17 February 2021 •
Published Online: 3 March 2021



View Online



Export Citation



CrossMark

Giovanni Manfredi,^{1,a)} Francesco Lodola,^{1,2} Giuseppe Maria Paternó,¹ Vito Vurro,^{1,3} Pietro Baldelli,^{4,5}
Fabio Benfenati,^{5,6} and Guglielmo Lanzani^{1,3}

AFFILIATIONS

¹Istituto Italiano di Tecnologia, Center for Nanoscience and Technology, Via Pascoli, 70, 20133 Milano, Italy

²Università degli studi di Milano-Bicocca, Dipartimento di Biotecnologie e Bioscienze, Piazza della Scienza, 2, 20126 Milano, Italy

³Politecnico di Milano, Dipartimento di Fisica, Piazza Leonardo da Vinci, 32, 20133 Milano, Italy

⁴Dipartimento di Medicina Sperimentale, Università di Genova, Viale Benedetto XV, 3, 16132 Genova, Italy

⁵Istituto Italiano di Tecnologia, Center for Synaptic Neuroscience and Technology, Largo Rosanna Benzi, 10, 16132 Genova, Italy

⁶IRCCS Ospedale Policlinico San Martino, Largo Rosanna Benzi, 10, 16132 Genova, Italy

Note: This paper is part of the Special Topic on Advances in Bioelectronics.

a) Author to whom correspondence should be addressed: giovanni.manfredi@iit.it

ABSTRACT

Cell membrane perturbation is a common way to stimulate cells by using external actuators. Recently, nanotechnology has added a number of new strategies for doing this, enlarging the scope and the range of mechanisms involved. Here, we describe a number of possible perturbation actions that are driven by light, and we try to capture the underlying phenomena. The discussion is based on the simple equivalent circuit model for the cell membrane.

© 2021 Author(s). All article content, except where otherwise noted, is licensed under a Creative Commons Attribution (CC BY) license (<http://creativecommons.org/licenses/by/4.0/>). <https://doi.org/10.1063/5.0037109>

INTRODUCTION

Many of the processes that rule the basic function, metabolism, and communication of living cells occur at the plasma membrane. Cell membranes are complex supramolecular aggregates, forming a barrier between compartments and harboring a variety of chemical reactions essential to the existence and functioning of a cell. Many proteins that regulate ion fluxes, energy exchange, cell adhesion, and movement are located at the cell membrane level. Here, in addition, a great part of cell homeostasis, signaling, and replication occurs. All these happen through a series of chemical reactions, mainly redox, phosphorylations, and condensations,¹ that are regulated by the transport of chemical compounds to and through the membrane itself.^{2,3} Recent studies also highlight the important role of cell membrane in aging of bacteria and in antibiotic resistance.^{4–7} Therefore, perturbing the dynamic equilibrium of the membrane may lead to cell stimulation and offer a handle for controlling cell activity. Here, we describe multiple approaches to pursue this goal, discussing the different physical perturbation mechanisms underlying each respective stimulating action.

Cell membranes have a thickness ranging between 4 nm and 10 nm and are constituted by a molecular assembly resulting from low-energy interactions occurring among a wide range of lipids and proteins.⁸ Phospholipids account for about half the mass of the cell membrane and are insoluble in water. In addition, due to their amphiphilic nature, lipids self-assemble into a double layer, with the non-polar hydrophobic tails facing each other in the bilayer core and the hydrophilic, polar phosphate heads in contact with water. In addition to lipids, membranes are loaded with proteins that play crucial roles in controlling cytoskeleton anchorage, cell to cell junctions, diffusion of ions and chemicals through channels and transporters, metabolic pathways, cell-to-cell identification, and receptor-dependent signaling. Depending on their structure, proteins can be embedded into the membrane (integral proteins) or loosely attached to its inside or outside face (peripheral membrane proteins and lipid-anchored proteins).⁸ The protein and lipid composition is specific to each cell type, even though it can change during cell replication as a strategy to avoid excessive defect replication and to enhance species survivability.^{4,6,7}

The accepted model that describes the membrane structure and dynamics is known as the fluid mosaic model and was first proposed by Singer and Nicolson in 1972.⁹ According to this model, lipids and proteins move easily in the membrane plane with a speed equal to micrometers per second and micrometers per minute, respectively. However, at the membrane level, there are domains capable of limiting the lateral diffusion of the molecules. It follows that the membrane does not have a uniform composition over the entire surface. This heterogeneity can be due to either the presence of particular regions, the so-called “rafts,” with a particular lipid and protein composition, or the interactions of membrane proteins with the underlying cytoskeleton.¹⁰ Although the fluid mosaic model has evolved over time, it still provides a good basic description of the structure and behavior of membranes in many cells.

The plasma membrane must fulfill two important functional tasks: (i) to protect the cell, acting as a barrier, and (ii) to ensure sufficient chemical communication between the intracellular and extracellular fluids, acting as a gatekeeper.¹¹ Transmembrane trafficking is associated with metabolism (e.g., nutrients) and functioning (ion fluxes able to depolarize or hyperpolarize the cell) in response to stimuli that propagate communication signals.

Physical models of the membrane, albeit oversimplified, aim at capturing essential features that govern its structure and function. Thermodynamics describes the different structural phases of the membrane at equilibrium and their transitions,¹² while fluid dynamics and electromagnetism provide the ingredients to describe membrane excitability and, in general, transient processes. In the following, we attempt a quick review of the latter.

THE ELECTRICAL PROPERTIES OF THE MEMBRANE

Cells generate a trans-membrane electric current by exchanging ions between their interior and their exterior. Interestingly, ion currents in cells and organelles obey the Ohm’s law to a certain extent, despite the complex structure involved in the current flow. Such a similarity to ohmic components allows describing the cell membrane using an equivalent electrical circuit composed of electromotive force (emf) generators, resistances, and capacitors as we will argue in the following.

In the lipid bilayer [Fig. 1(a)], the membrane core is mostly composed of the hydrophobic phospholipid tails, exhibiting a relatively low dielectric constant (around 2–3),¹³ while the polar heads that are interfacing with either the extracellular or the cytoplasmic fluid (in the outer and inner leaflet, respectively) possess a dielectric constant close to that of water (about 80).¹³ The lipid bilayer is practically impermeable to ions, as the energy necessary to cross the two phases (hydrophobic membrane interior and external aqueous environment) and the membrane itself is in the order of some eV,¹⁴ meaning that under ordinary conditions, ions cannot pass from the aqueous solution to the hydrophobic part of the membrane. Ionic current through pure lipid membranes has been shown to occur only under the influence of strong transmembrane electric fields (electroporation) or as a result of structural rearrangements of the lipid bilayer during phase transition (soft perforation).¹⁵ According to such an observation, the electrical conductance of a lipid bilayer should be basically negligible ($\sim 10^{-13}$ S/m²); however, electrical measures on cell membranes show that its conductance is small but not inappreciable.¹³ Such an anomaly suggests that there is another mechanism, allowing ionic trafficking between the cell exterior and the cell interior. This role is indeed assumed by specific membrane proteins, ion channels, and ion pumps, which form passive or active percolating pathways to ions. It is thus clear that the concept of electrical resistance in the equivalent circuit is a lump sum of a complex multitude of processes concurring to the membrane conductance.

While the membrane conductivity is, principally, related to proteins, its electrical capacitance, instead, is straightly dependent on the membrane lipidic part. Assuming the structure indicated in Fig. 1(a), one can use the simple plate capacitor equation for estimating the cell specific capacitance $C = \epsilon/h$ (with ϵ being the electrical permittivity and h being the membrane thickness). A typical capacitance value for the lipid membrane is in the order of $1 \mu\text{F}/\text{cm}^2$,¹⁶ well in agreement with the experimentally observed capacitance in live cells. This means that the effect of the phospholipid layer *per se* accounts for the capacitance observed in a whole cell, while channels, transporters, and other membrane proteins do not significantly affect the capacitance value.

In addition, the membrane acts as an electric generator able to keep a specific voltage difference across the membrane itself. Indeed, it is well known that the cytosolic ionic concentrations are different

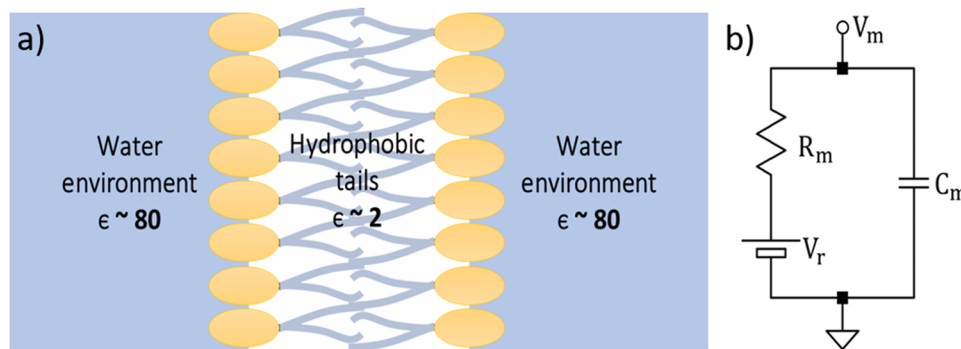


FIG. 1. (a) Cartoon depicting the membrane structure. (b) Schematic diagram of the equivalent circuit model of the membrane.

from those of the extracellular environment. In particular, in their interior, cells are poor in Na^+ , Cl^- , and Ca^{2+} , while being enriched in K^+ .¹⁷ This ionic gradient is maintained by specific proteins called ion pumps, and it is responsible for generating an electrochemical gradient across the two sides of the membrane.

The potential difference across the plasma membrane (membrane potential, V_m) typically varies between -20 mV and -100 mV. Such a potential arises from an electric asymmetry on the two sides of the membrane, as the result of both active electrogenic pumping and passive ion diffusion. In mammalian cells, the K^+ gradient, generated by using the Na^+/K^+ pump, has a major influence on the membrane potential because of the prevalence of passive K^+ diffusion.

Under this condition, a fundamental law, the Nernst equation, quantitatively expresses the equilibrium state in which there is no net flow of ions across the plasma membrane,

$$V_m = \frac{RT}{F} \ln \frac{[\text{K}^+]_O}{[\text{K}^+]_I}, \quad (1)$$

where R is the gas constant, T is the temperature, F is the Faraday constant, and the subscripts "O" and "I" indicate the K^+ concentration outside and inside the membrane, respectively. Although the K^+ gradient always has a major influence on the membrane potential, the presence of a significant passive diffusion for other ions (Na^+ and Cl^-) in most cells significantly affects it.

Under this condition, we could state that the more permeable the membrane for a given ion, the more the membrane voltage approaches the equilibrium value for that ion. The equation dictating such a scenario, considering only the most important monovalent ions, is the Goldman-Hodgkin-Katz (GHK) equation,¹⁸

$$V_m = \frac{RT}{F} \ln \left(\frac{p_K[\text{K}^+]_O + p_{\text{Na}}[\text{Na}^+]_O + p_{\text{Cl}}[\text{Cl}^-]_I}{p_K[\text{K}^+]_I + p_{\text{Na}}[\text{Na}^+]_I + p_{\text{Cl}}[\text{Cl}^-]_O} \right), \quad (2)$$

where p_i is the membrane permeability of ion "i" and the subscripts "O" and "I" indicate the ion concentration outside and inside the membrane, respectively. The membrane voltage is called the resting potential (V_r) when the voltage difference across a membrane is not perturbed by the ionic flux through active channels.

A complete representation of the membrane should also account for the presence of ions adsorbed over the hydrophilic dipolar heads of the membrane lipids. Indeed, the electrical dipole present on the phospholipid head induces the accumulation of positive ions.^{19–21} The resulting surface charge density, typically ranging from 0.002 C/m² to 0.3 C/m², approximately follows the Langmuir adsorption model, with an estimated binding energy in the range $U/K_B T \approx 1–10$. Hence, the surface charge depends on the ionic concentration of the electrolytic solutions across the membrane. If the external and internal compartments have equal ion concentrations, the charges are symmetrically loaded on the two membrane leaflets and do not cause a voltage difference across the membrane. Vice versa, when the adsorbed ions are asymmetrically loaded on the two membrane leaflets, the charge unbalance generates an electric field inside the membrane. The magnitude of this field is very high, in the order of 10^7 V/m– 10^9 V/m. Such a large field could, in principle,

play a role in the cell membrane stability. However, its effects are rarely considered due to the very strong shielding caused by the ionic solution. Indeed, the Debye length of these systems is in the order of 1 nm. Similarly, they are not considered in experiments because the typical stimuli are far too weak to affect the surface charge. Note that the presence of tightly bounded charges onto the membrane leaflets poses a strain onto the membrane structure, due to the coulomb repulsion among surface charges, that can reach thousands of atmospheres. This electro-mechanical stress contributes to the thermodynamic equilibrium of the bilayer and affects the transition temperature.²²

Overall, the membrane can be electrically described with the scheme in Fig. 1(b). Its components typical values are reported in Table I. The resistance R_m is an average value that keeps into account the contribution of all the ions participating in the current flow, with different ions possessing different Nernst potentials [Eq. (1)]. This is at the base of the GHK equation [Eq. (2)], and it can be introduced in the equivalent circuit by adding branching for each ion with a resistance R_k (or conductance g_k) and a battery E_k .²³

The equivalent circuit of Fig. 1(b) allows for capturing the essential physical phenomena that are involved in the optostimulation process. The membrane voltage is represented by the difference in the potential between the two sides of the membrane capacitor, as expressed by the following equation:

$$V_m = Q_m/C_m, \quad (3)$$

where Q_m is the quantity of charge stored at the two membrane interfaces and C_m is the membrane capacitance. At the resting state, only passive ion diffusion is present; thus, $V_m = V_r$, and the net current flowing through the membrane is 0. On the other hand, when physiological changes occur, a current due to opening or closing of channels will flow across the membrane and its voltage will change. In particular, it will increase (depolarization) if a net positive charge flows inside the cell (inward current) or decrease (hyperpolarization) if a net positive charge flows outside the cell (or a negative charge flows inside the cell; outward current). We will now synthetically explain what happens upon modulation of one of the three parameters of the equivalent circuit reported in Fig. 1(b) on different time scales, while keeping the others constant. To do this, we will examine the cases of a sudden or slow and linear variation in capacitance, resistance, or voltage. The two types of change follow the curves of Figs. 2(a) and 2(e), which are represented in scale of the basal values $C_m^0 = 30$ pF, $R_m^0 = 500$ M Ω , and $V_r^0 = -30$ mV, respectively. All the three parameters are individually varied between 1 and 1.1 times their initial value.

TABLE I. Major responsible elements for membrane electrical properties and typical values.

	Conductance	Capacity	Potential generation
Major responsible element	Proteins	Lipids	Proteins
Typical values	100 S/m ²	1 μ F/cm ²	10 mV–100 mV

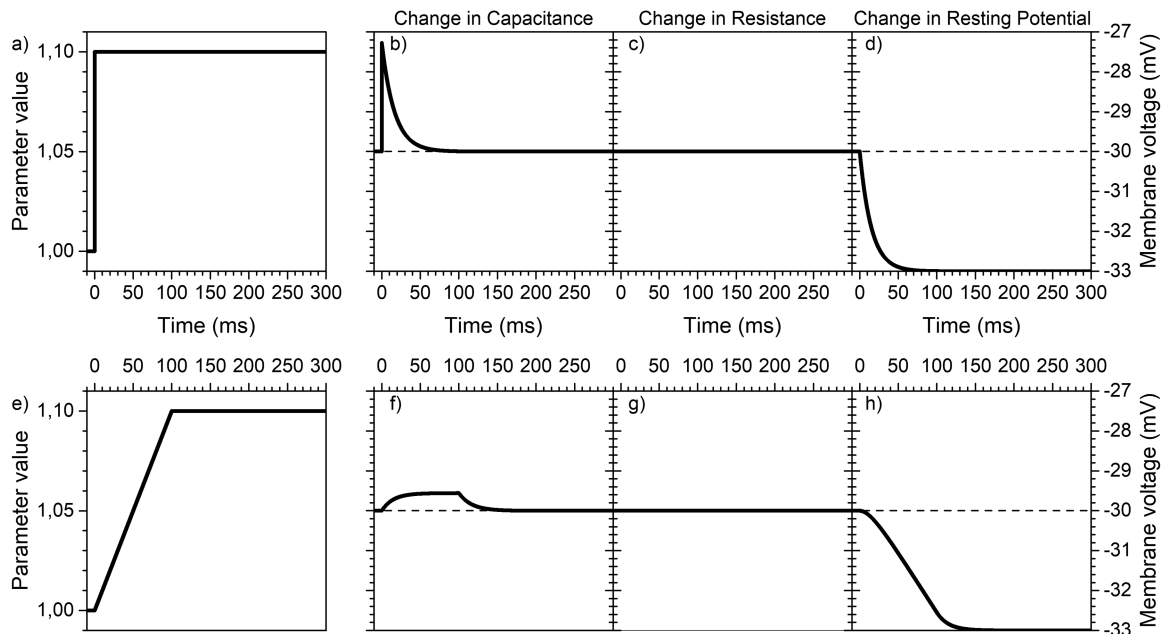


FIG. 2. Representative curves of membrane voltage evolution after variation of one of the constituents of a membrane equivalent circuit. Considered parameters are $R_m^0 = 500 \text{ M}\Omega$, $C_m^0 = 30 \text{ pF}$, and $V_r^0 = -30 \text{ mV}$. Each one between R_m , C_m , and V_r is varied according to time evolution (a) or (e). At $t = 0$, the considered variable is always at its initial value. In (a), there is an immediate ($Dt = 1 \text{ ms}$) jump from 1 to 1.1. (b), (c), and (d) Variation of membrane voltage after the capacitance, resistance, or resting potential, respectively, are varied according to curve (a). (f), (g), and (h) Variation of membrane voltage after the capacitance, resistance, or resting potential, respectively, are varied according to curve (e) ($Dt = 100 \text{ ms}$).

Capacitance

If a sudden change in capacitance occurs, the membrane voltage quickly changes according to the capacitor potential equation [Eq. (3)], given that the amount of charge stored on the two sides of the membrane (Q_m) will initially remain constant. The voltage change will result in a displacement current until the potential goes back to its resting value and the charge accumulated on the capacitor is readjusted accordingly [Fig. 2(b)]. Such a dynamics has a characteristic relaxation time $\tau_m = R_m \cdot C_m$ that is typically in the millisecond time scale. Alternatively, if the change in capacitance is slow, the effect will consist in a convolution between the variation of capacitance and the voltage relaxation to the resting potential, as the relaxation time τ_m will also be varying in time. The behavior is depicted in Fig. 2(f). The maximum variation in the membrane potential will be linked to the speed of the capacitance change.

Resistance

At equilibrium, there is no current in the equivalent circuit. Consequently, changes in the passive membrane resistance (R_m) do not result in any variation of the membrane potential [Figs. 2(c) and 2(g)]. On the other hand, membrane resistance has an impact on the relaxation time constant τ_m , meaning that the processes kinetics will be different upon the variation of the equilibrium conditions, i.e., due to modulation of membrane voltage and/or membrane capacitance.

Resting potential

A sudden change in the battery potential (i.e., the resting potential) does not initially change the membrane potential. This will evolve to a new equilibrium value slowly in time, according to the characteristic time constant of the equivalent circuit [Fig. 2(d)]. When the change in the resting potential is not immediate, the membrane potential response will be the convolution of a relaxation from the starting value to the varying V_r that will eventually plateau after the latter reaches a constant value [Fig. 2(h)]. Note that a change in emf can lead to permanent changes in the resting potential value, in contrast with what happens upon the variation of the capacitance, where there is always a relaxation back to the starting resting potential.

ROLE OF THE EXOGENOUS PHYSICAL STIMULI

In this section, we will introduce the most popular techniques used to perturb biological membranes and discuss about their effects on the equivalent circuit parameters.

Current injection

A current I_0 injected across the membrane initially induces the displacement of charges on the capacitor. The potential difference changes according to $V(t) = I_0 \cdot R_m \cdot (1 - e^{-\frac{t}{\tau}})$ until it compensates the voltage drop reaching $V_m = I_0 \cdot R_m$.

Such a change in voltage can induce the opening or closing of voltage sensitive channels,²⁴ which, in turn, shifts the resting potential of the cell (by changing the membrane permeability, R_m). Depending on the type of channels present in the membrane, such an opening can trigger cascade mechanisms like the ones that lead to action potential firing in excitable cells.

In standard electrophysiology, current injection is typically obtained by using the patch-clamp electrode in the current-clamp or voltage-clamp mode. Alternatively, inward or outward current flows can be related to the drug induced opening of an ion channel in response to a specific stimulus. Less invasive techniques more relevant here are based on the use of microelectrodes or flat contacts that, when polarized, support a current to a counter electrode usually nearby. Electrodes of many different shapes have been tested, including needles, dots, or mushroom-like hemispheres.^{25,26} The geometry of the circuit controls the space resolution that can be achieved by this stimulation. The use of electrical stimulation by current injection is well established, especially *in vivo*.^{27,28} Yet, it bears a number of drawbacks, such as the limited space resolution due to current spreading, the fading in time of the efficiency due to electrode degradation, inflammation reactions and the detrimental effect of the current flow through tissues, that generate reactive oxygen species (ROS).

Electric field

A static electric field across the biological membrane acts with a force upon the ions. It makes a difference to consider mobile ions or adsorbed ions. About the former, their motion under the field can be rationalized as a current flowing in the circuit. The potential across the membrane will change as long as the external stimulus is applied. As in the case of current injection, the voltage change can induce a response in voltage sensitive channels and potentially trigger cascade mechanisms, leading to membrane potential polarization.

If the applied electric field is strong enough, it could also interact with the physically adsorbed surface ions. For instance, the field could strip some of the ions, changing the equilibrium between adsorption and desorption. A possible scenario is the presence of a photoinduced *negative* charge adjacent to the membrane, for instance, supported by excited nanoparticles. The field could preferentially strip a positive ion away from the closer side and enhance the accumulation on the opposite side of the membrane. This unbalance would change the intramembrane electrical field, leading to local effects, which could potentially affect membrane stability or induce conformational changes in membrane proteins sensitive to the electric field, such as voltage-dependent ion channels. Another phenomenon, suggested by Heimburg,²² is the reduction in the phase transition temperature of the membrane by the electric field. Under physiological conditions, this could be enough for triggering a phase transition.

Electrostatic perturbation can be achieved by capacitive coupling through an electrode or a photo-electrode placed adjacent to the membrane, forming a cleft of 10 nm–100 nm. Charge accumulates at the electrode surface and generates the perturbing electric field whose effect on the membrane depends on the coupling efficiency. The latter is mainly limited by the electrical conductivity of the cleft whose size and composition are, however, hard to be known. Even if a precise tailoring is not possible, there is a

general consensus on the role of the interface geometry and a plethora of examples have been reported in the literature, including silicon nanorods,²⁹ conjugated polymers nanostructures,^{30–33} carbon nanotubes,³⁴ and inorganic semiconductor nanostructures.^{35,36}

Variation of membrane dielectric environment

A small change in the dielectric function ϵ , which does not lead to drastic changes in membrane interfacial energy or pore formation, may still affect the capacitance as described by the following equation:

$$\frac{dC}{C} = \frac{d\epsilon}{\epsilon}. \quad (4)$$

In this case, the overall consequence will be a transient change in membrane voltage with a return to equilibrium, as shown in Figs. 2(b) and 2(f). Note that the change in the dielectric function can also be a consequence of a change in temperature, as discussed below. The change in the dielectric environment of the lipid membrane also has an impact on the partition energy and, thus, on the membrane permeability. This condition can be achieved via the insertion of exogenous molecules in the membrane.³⁷ Notably, a variation in the dielectric function can also affect the folding of trans-membrane proteins. The transient change in membrane voltage, which is expected when the dielectric permittivity variation is induced by molecules percolating inside the lipid bilayer,³⁸ can lead to opening or closing of active channels.

Mechanical strain on the membrane

In general, we can assume that the membrane can undergo two main effects when subjected to a mechanical strain, namely, stretching/shrinking and thinning/thickening. Note that according to a simple continuum elastic model, the two effects strictly correlate. The change in thickness induces a variation in the membrane capacitance following the law

$$\frac{dC}{C} = \left(-\frac{1}{h} + \frac{1}{\epsilon} \frac{\partial \epsilon}{\partial h} \right) dh. \quad (5)$$

The dielectric function depends on the density; this, in turn, introduces a dependence of ϵ on membrane thickness that is additional to the change in geometry. However, the latter effect is usually small and can be neglected, meaning that an increase/decrease in thickness is inversely related to capacitance, in accordance to the $1/h$ dependence and in the absence of any other concomitant effect (i.e., modification of the membrane permeability and integrity).

The use of photo-mechano-transducers exploiting the steric hindrance change has been exploited effectively for modulating the membrane capacitance in both model membranes and living cells. An important family of photo-mechano-transducers is represented by azobenzene derivatives, which photoisomerize between the elongated *trans* isomer and the bent *cis* isomer under UV–Vis light illumination.³⁹ Fujiwara and Yonezawa tested an aliphatic amphiphilic azobenzene derivative to change the capacitance of black lipid membranes in response to prolonged (several seconds) ultraviolet illumination.^{40,41} They obtained a permanent modification of their membrane state; however, to our knowledge, their molecules were not tested in living cells. Recently, the effect of a new amphiphilic

azobenzene was reported. Such an actuator dwells into the plasma membrane in a non-covalent manner. Upon illumination for 10 ms–100 ms with visible light, they induce transient hyperpolarization followed by delayed depolarization in neurons, triggering action potential firing both *in vitro* and *in vivo*.^{42,43} The optomechanical stimulation mechanism resides in the *trans* → *cis* photoreaction of azobenzenes that results in membrane thinning/thickening, possibly due to a supramolecular phenomenon. Such an effect has also been validated by several experimental techniques, including neutron scattering.⁴⁴ Specifically, in the dark, the elongated *trans* isomers can dimerize, causing a thinning of the membrane and an increase in its electrical capacitance, while illumination triggers the formation of a stable population of bent *cis* isomers. Thus, the disruption of the dimers leads to restoration of membrane thickness and capacitance. Overall, these resemble molecular machines mimicking the opening and closing of a clip.

Mechanical perturbation of the lipid membrane has also been achieved via the insertion of amphiphilic conjugated oligo electrolytes (COEs)^{45,46} that exploit Coulomb interaction between ions in the dark. Upon insertion, COEs structurally distort the membrane, as the lipid phosphate heads are drawn toward the center of the bilayer by the cationic groups of the COE structures.⁴⁷ In contrast to the capacitance modulation mechanism, such an approach has been found to facilitate the transmembrane movement of ions across mammalian membrane patches⁴⁸ and decrease the electrical resistance of *Escherichia coli* cells.⁴⁹ There is yet no evidence of a light triggered response based on this type of phenomenon.

Other effects that can occur upon application of mechanical strains are linked to the response of ion channels and pumps. Indeed, it is known that in some membranes, both the resistance and the resting potential can change upon the application of a mechanical strain^{50,51} owing to the presence of specific mechanosensitive channels.⁵²

Activation or inactivation of ion pumps

Pumps are active proteins that balance chemical concentrations on the two sides of the membrane. Some pumps are responsible for potentially harmful compounds' expulsion from cells and take an active role in antibiotic resistance.^{7,53,54} Others, instead, affect ion concentrations inside the cell and keep a gradient between the inside and the outside. Such a gradient is responsible for the formation of a Nernst potential and can be used in the GHK equation [Eq. (2)], which can be rewritten as follows:

$$V_r = \frac{RT}{F} \ln \left(\frac{\sum P_A [A^+]_O + \sum P_B [B^-]_I}{\sum P_A [A^+]_I + \sum P_B [B^-]_O} \right). \quad (6)$$

The typical volume of a cell is in the order of picoliters or less, while the extracellular medium is typically a much larger volume *in vitro*. The difference in volume is order of magnitudes, and this allows us to reasonably assume that ion pumps of one cell can only alter the ionic concentration of the cytosol, leaving basically unchanged the extracellular medium. Hence, focusing on the variation of only one ionic species (i.e., a positive ion X^+), the derivative becomes

$$\frac{dV_r}{d[X^+]_I} = - \frac{RT}{F} \frac{\sum P_A [A^+]_O + \sum P_B [B^-]_I}{\sum P_A [A^+]_I + \sum P_B [B^-]_O} P_X [X^+]_I. \quad (7)$$

A permanent variation in the *activation/inactivation* mechanism of ion pumps leads to a constant change in the membrane resting potential.

In this regard, research in optogenetics has identified and developed the light-driven chloride pump halorhodopsin from *Natronomonas pharaonis* and the light-driven proton pump archaeorhodopsin from *Archaeobacteria* that under illumination generate outward currents for the temporally precise optical inhibition of neural activity.⁵⁵

Closing or opening of ion channels

Similar to ionic pumps, the channels allow for the passage of ions through the membrane, but, different from pumps that move ions creating a gradient, channels can let ions cross the membrane along the electrochemical gradient generated by the pumps. Ion channels can be passive structures that allow for the passage of ionic current on the basis of the electrochemical gradient or active structures that open in response to a variety of stimuli such as changes in the membrane potential, neurotransmitters released at the synaptic level, the stretch of the membrane, and physical–chemical stimuli of the extracellular (H^+ concentration, temperature) or intracellular (second messengers, phosphorylation) media.

Ion channels opening/closing have a strong impact on membrane permeability. In particular, assuming that these channels are able to maintain a constant ionic concentration difference across the membrane, an assumption that is generally valid unless during the occurrence of an action potential, the change in the permeability can be treated using the GHK equation [Eq. (2)] that, for a variation in permeability of cation X, can be adapted in the following expression:

$$\frac{dV_r}{dP_X} = \frac{RT}{F} P_X \left(\frac{[X^+]_O}{\sum P_A [A^+]_I + \sum P_B [B^-]_O} - \frac{[X^+]_I}{\sum P_A [A^+]_O + \sum P_B [B^-]_I} \right). \quad (8)$$

The global effect is then a change in both the membrane resting potential and resistance, which leads to a constant shift in the membrane potential.

An ion channel can be “gated” in a large variety of ways, which are well documented in the literature. A common way to affect the ion channel status is to change the membrane potential. Depolarization leads to ion channel opening (voltage gated channels), and often fundamental processes spring from this initial step. Counter-intuitively, hyperpolarization may also lead to ion channel opening and eventually depolarization as in the case of hyperpolarization-activated and cyclic nucleotide-gated (HCN) channels. Other natural phenomena can be mimicked by artificial stimuli, such as chemical or pharmacological gating. Those stay in the more standard biotechnology toolbox and should not be considered here. However, it is worth noting the recent development of artificial neurotransmitter (ions) pumps based on organic bio-electronics.^{56,57} Two other effective approaches are optogenetics—which induce the expression of artificial ion channels that can be controlled by light⁵⁸—and covalent attachment of photochromic molecules to ion channels that drives opening or closing upon isomerization.^{59–61}

Temperature variations

A change in temperature (T) can act on all the electrical properties of the membrane equivalent circuit, not considering other specific effects such as T -dependent ion channels. Capacitance, resistance, and voltage follow empirical laws as described below.

Capacitance increases linearly with temperature, at least for small variations, in accordance with the universal rate equation $\Delta C/C = \alpha \Delta T$, with $\alpha = 0.003 \text{ K}^{-1}$.^{62,63} This behavior is unexpected, as heating should, in principle, lead to thermal expansion, thus causing an increase in membrane thickness and a reduction in capacitance. Even when considering the ion distributions on the two sides of the membrane, as described by the coupled Boltzmann and Poisson equation,¹⁹ the increase in temperature leads to a reduction in capacitance. The experimental observation is thus pointing out a different phenomenon, generically assigned to a phase transition in the membrane that becomes thinner with a larger area, upon increasing the temperature.

The membrane resistance follows the exponential law,^{63,64}

$$R_m = R_m^0 Q_{10}^{-\frac{T-T_0}{10}}, \quad (9)$$

where Q_{10} is an empirical parameter. From Eq. (9), we see that an increase in temperature brings to a reduction in membrane resistance.

The resting potential follows a power law,⁶³

$$V_r = V_r^0 \left(\frac{T}{T_0} \right)^{\alpha_v}, \quad (10)$$

where α_v is again an empirical parameter, typically smaller than 1. An increase in temperature leads to an increase in the absolute value of the membrane potential. The resting potential being typically negative means that high temperatures lead to hyperpolarization.

In Fig. 3, we show the prototypical behavior of the membrane potential in a model cell subjected to a temperature rise. For a sudden change in temperature [Figs. 3(a) and 3(b)], the cell initially depolarizes due to the change in capacitance. This process relaxes back to equilibrium with the characteristic membrane time constant. Concomitantly, the increase in baseline temperature causes resting potential hyperpolarization according to the GHK equation [Eq. (2)]. In typical real cases, heat stimuli are supplied by pulsed laser excitation. These kinds of stimuli resemble the ones shown in Fig. 3(c). A fast rise in temperature to a plateau occurring in the time scale of tens of milliseconds is followed by a slower cooling. Under such conditions, the membrane voltage [Fig. 3(d)] initially rises (depolarization) due to the capacitance increase, as already discussed, and subsequently relaxes to the new resting potential, which is typically lower than the initial one (hyperpolarization). When heating stops and the cool-down begins, a slow relaxation to the initial resting potential returning to the start state occurs. Such

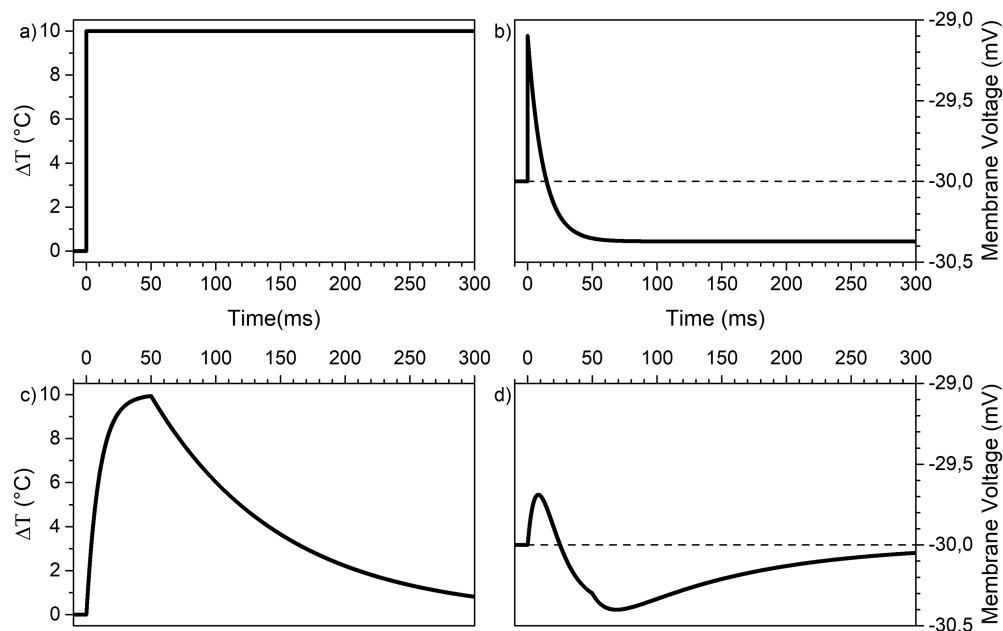


FIG. 3. Representative curves of membrane voltage evolution after temperature variations. The cell parameters were set at $R_m^0 = 500 \text{ M}\Omega$, $C_m^0 = 30 \text{ pF}$, and $V_r^0 = -30 \text{ mV}$. The temperature varies according to curves (a) and (c). In the case of a sudden temperature change, the membrane voltage (b) first increases (depolarization), due to the increase in capacitance, and then decays to a new resting voltage, which is less than the initial state (hyperpolarization). When the temperature variation is slow as in (c), the membrane voltage variation (d) is a convolution between the sudden behavior and the slow variation of temperature and depends on the time constant ($\tau = RC$) of the system.

simulation well-reproduces what is observed in HEK cells lying on top of a photoexcited conjugated polymer film.⁶³ We note here that a rise in temperature could reduce the adsorption, favoring desorption of fixed ions at the membrane phospholipids heads. This would lead to a change in the electrostatic strain onto the hydrophobic membrane core, reducing the thickness. This mechanism could contribute to the membrane thinning upon rising the temperature.

Local temperature variations to induce biological effects have been considered since long ago. Infrared radiation can deposit energy into the cell medium and lead to local heating.⁶² Infrared requires high intensity, in the order of 10 W/mm². Temporal and spatial thermal confinement is necessary to achieve neuronal stimulation while reducing tissue damage.⁶⁵ This requires optical pulses longer than 500 ns and shorter than 200 ms. Infrared-induced activation seems to be due to a brief spatiotemporal thermal gradient, whereas neuron silencing is assigned to an increase in the baseline temperature,⁶⁶ according to the above discussion. This method can be spatially imprecise due to the non-localized water absorption process, an effect that can also lead to long-term photodegradation effects, likely driven by ROS production. For these reasons, various light-to-heat nanotransducers that are able to spatially confine the thermal effect have been introduced recently.⁶¹ Note that we exclude here thermal dynamic therapy and stay focused on mild effect aimed at cell stimulation and not at cell death. Given their easy delivery through injection, their optical properties, and their tunability, nanoparticles are the most interesting actuators for cell thermal stimulation. Typically, metallic dots such as gold nanoparticles are used.^{67,68} Here, the surface plasmon photoexcitation is exploited to convey large amounts of energy to electrons that quickly thermalize realizing energy to the metal lattice, thus leading to a temperature rise.⁶⁹ The required light intensity can be very high, in the 100 W/mm² range. Visible light penetration is limited to few mm from the surface due to absorption and scattering. To overcome such a limitation, particles that heat up due to an oscillating magnetic field are also considered,⁷⁰ bringing the advantage of deep stimulation into a tissue.

CONCLUSIONS

To summarize, an equivalent circuit containing effective electrical components seems to be a useful and simple physical model able to capture the essential features of cell stimulation via membrane perturbation. The model correctly predicts the effect of external stimulation, provided that the specific effect on each component is known, although such a reductionist approach does not fully explain the occurrence of certain physiological phenomena, as in the case of the thermal increase in capacitance. A reasonable speculation is that this can be due to a phase transition in the membrane structure. Here, we speculate that fixed ions adsorbed at the membrane may play a role too. Recent developments using molecular intramembrane switches open new ways to obtain cell stimulation by low invasiveness membrane perturbation. A deep understanding of the membrane physics through the study of new membrane actuation mechanisms will lead to the development of the next generation biotic/abiotic interfaces for application in artificial organs and brain machine interfaces.

ACKNOWLEDGMENTS

We acknowledge Fondazione Cariplo (Grant Nos. 2018-0979 and 2018-0505) and H2020-MSCA-ITN 2019 “Entrain Vision” (Project No. 861423) for financial support.

DATA AVAILABILITY

Data sharing is not applicable to this article as no new data were created or analyzed in this study.

REFERENCES

- D. L. Nelson, M. M. Cox, and A. L. Lehninger, *Lehninger Principles of Biochemistry*, 7th ed., International edition (W. H. Freeman, New York NY, 2017).
- M. I. Monine and J. M. Haugh, *J. Chem. Phys.* **123**(7), 074908 (2005).
- T. Rosenberg and W. Wilbrandt, *Exp. Cell Res.* **9**(1), 49 (1955).
- U. Lapińska, G. Glover, P. Capilla-Lasheras, A. J. Young, and S. Pagliara, *Philos. Trans. R. Soc., B* **374**(1786), 20180442 (2019).
- J. Vergalli, E. Dumont, J. Pajović, B. Cinquin, L. Maigre, M. Masi, M. Réfrégiers, and J.-M. Pagès, *Nat. Protoc.* **13**(6), 1348 (2018).
- J. Vergalli, E. Dumont, B. Cinquin, L. Maigre, J. Pajovic, E. Bacqué, M. Mourez, M. Réfrégiers, and J.-M. Pagès, *Sci. Rep.* **7**(1), 9821 (2017).
- T. Bergmiller, A. M. C. Andersson, K. Tomasek, E. Balleza, D. J. Kiviet, R. Hauschild, G. Tkačik, and C. C. Guet, *Science* **356**(6335), 311 (2017).
- A. Uzman, *Biochem. Mol. Biol. Educ.* **31**(4), 212 (2003).
- S. J. Singer and G. L. Nicolson, *Science* **175**(4023), 720 (1972).
- E. Sezgin, I. Levental, S. Mayor, and C. Eggeling, *Nat. Rev. Mol. Cell Biol.* **18**(6), 361 (2017).
- J. Bernardino de la Serna, G. J. Schütz, C. Eggeling, and M. Cebecauer, *Front Cell Dev. Biol.* **4**, 106 (2016).
- T. Heimburg, *Thermal Biophysics of Membranes*, 1 ed. (Wiley, 2007).
- H. G. L. Coster, *J. Biol. Phys.* **29**(4), 363 (2003).
- B. Neumcke and P. Läuger, *Biophys. J.* **9**(9), 1160 (1969).
- B. Wunderlich, C. Leirer, A. L. Idzko, U. F. Keyser, A. Wixforth, V. M. Myles, T. Heimburg, and M. F. Schneider, *Biophys. J.* **96**(11), 4592 (2009).
- J. Golowasch and F. Nadim, in *Encyclopedia of Computational Neuroscience*, edited by D. Jaeger and R. Jung (Springer, New York, NY, 2014), p. 1.
- H. Lodish, A. Berk, S. L. Zipursky, P. Matsudaira, D. Baltimore, and J. Darnell, *Molecular Cell Biology*, 4th ed. (W. H. Freeman, New York, 2000), p. 1084.
- A. L. Hodgkin and B. Katz, *J. Physiol.* **108**(1), 37 (1949).
- M. Plaksin, E. Shapira, E. Kimmel, and S. Shoham, *Phys. Rev. X* **8**(1), 011043 (2018).
- Y. Ma, K. Poole, J. Goyette, and K. Gaus, *Front. Immunol.* **8**, 1513 (2017).
- M. Pekker and M. N. Shneider, *J. Phys. Chem. Biophys.* **5**(2), 177 (2015).
- T. Heimburg, *Biophys. J.* **103**(5), 918 (2012).
- F. Gabbiani and M. J. Cox, *Mathematics for Neuroscientists*, 1st ed. (Elsevier, Academic Press, Amsterdam, 2010), p. 486.
- D. Purves, G. J. Augustine, D. Fitzpatrick, L. C. Katz, A.-S. LaMantia, J. O. McNamara, and S. M. Williams, *Neuroscience*, 2nd ed. (Sinauer Associates, Sunderland, Mass, 2001), p. 681.
- A. Fendyur, N. Mazurski, J. Shappir, and M. E. Spira, *Front. Neuroeng.* **4**, 14 (2011).
- S. M. Ojovan, N. Rabieh, N. Shmoel, H. Erez, E. Maydan, A. Cohen, and M. E. Spira, *Sci. Rep.* **5**(1), 14100 (2015).
- P. Fromherz, “Neuroelectronics interfacing: Semiconductor chips with ion channels, cells and brain,” in *Nanoelectronics and Information Technology*, edited by R. Weise (Wiley-VCH, Berlin, 2003), pp. 781–810.
- P. Fromherz and A. Stett, *Phys. Rev. Lett.* **75**(8), 1670 (1995).
- R. Parameswaran, J. L. Carvalho-de-Souza, Y. Jiang, M. J. Burke, J. F. Zimmerman, K. Koehler, A. W. Phillips, J. Yi, E. J. Adams, F. Bezanilla, and B. Tian, *Nat. Nanotechnol.* **13**(3), 260 (2018).

- ³⁰N. A. Lüdmilla Chenais, M. J. I. Airaghi Leccardi, and D. Ghezzi, *J. Neural Eng.* **18**, 016016 (2019).
- ³¹N. Martino, D. Ghezzi, F. Benfenati, G. Lanzani, and M. R. Antognazza, *J. Mater. Chem. B* **1**(31), 3768 (2013).
- ³²D. Ghezzi, M. Rosa Antognazza, M. Dal Maschio, E. Lanzarini, F. Benfenati, and G. Lanzani, *Nat. Commun.* **2**, 166 (2011).
- ³³J. F. Maya-Vetencourt, G. Manfredi, M. Mete, E. Colombo, M. Bramini, S. Di Marco, D. Shmal, G. Mantero, M. Dipalo, A. Rocchi, M. L. DiFrancesco, E. D. Papaleo, A. Russo, J. Barsotti, C. Eleftheriou, F. Di Maria, V. Cossu, F. Piazza, L. Emionite, F. Ticconi, C. Marini, G. Sambuceti, G. Pertile, G. Lanzani, and F. Benfenati, *Nat. Nanotechnol.* **15**, 698 (2020).
- ³⁴L. Bareket, N. Waiskopf, D. Rand, G. Lubin, M. David-Pur, J. Ben-Dov, S. Roy, C. Eleftheriou, E. Sernagor, O. Cheshnovsky, U. Banin, and Y. Hanein, *Nano Lett.* **14**(11), 6685 (2014).
- ³⁵T. C. Pappas, W. M. S. Wickramanyake, E. Jan, M. Motamedi, M. Brodwick, and N. A. Kotov, *Nano Lett.* **7**(2), 513 (2007).
- ³⁶K. Lugo, X. Miao, F. Rieke, and L. Y. Lin, *Biomed. Opt. Express* **3**(3), 447 (2012).
- ³⁷J. Dilger, S. McLaughlin, T. McIntosh, and S. Simon, *Science* **206**(4423), 1196 (1979).
- ³⁸Y. Hayashi, L. Livshits, A. Caduff, and Y. Feldman, *J. Phys. D: Appl. Phys.* **36**(4), 369 (2003).
- ³⁹H. M. D. Bandara and S. C. Burdette, *Chem. Soc. Rev.* **41**(5), 1809 (2012).
- ⁴⁰Y. Yonezawa, H. Fujiwara, and T. Sato, *Thin Solid Films* **210-211**, 736 (1992).
- ⁴¹H. Fujiwara and Y. Yonezawa, *Nature* **351**, 724 (1991).
- ⁴²M. L. DiFrancesco, F. Lodola, E. Colombo, L. Maragliano, M. Bramini, G. Maria Paternò, G. M. Paternò, P. Baldelli, M. D. Serra, L. Lunelli, M. Marchioretto, G. Grasselli, S. Cimò, L. Colella, D. Fazzi, F. Ortica, V. Vurro, J. F. Maya-Vetencourt, C. G. Eleftheriou, D. Shmal, and J. F. Maya-Vetencourt, C. Bertarelli, G. Lanzani, and F. Benfenati, *Nat. Nanotechnol.* **15**(4), 296 (2020).
- ⁴³G. Maria Paternò, E. Colombo, V. Vurro, F. Lodola, S. Cimò, V. Sesti, E. Molotokaite, M. Bramini, L. Ganzer, D. Fazzi, C. D'Andrea, F. Benfenati, C. Bertarelli, and G. Lanzani, *Adv. Sci.* **7**(8), 1903241 (2020).
- ⁴⁴G. M. Paternò, G. Bondelli, V. G. Sakai, V. Sesti, C. Bertarelli, and G. Lanzani, *Langmuir* **36**(39), 011517 (2020).
- ⁴⁵S. R. McCuskey, Y. Su, D. Leifert, A. S. Moreland, and G. C. Bazan, *Adv. Mater.* **32**(24), 1908178 (2020).
- ⁴⁶B. Wang, B. N. Queenan, S. Wang, K. P. R. Nilsson, and G. C. Bazan, *Adv. Mater.* **31**(22), 1806701 (2019).
- ⁴⁷H. Yan, C. Catania, and G. C. Bazan, *Adv. Mater.* **27**(19), 2958 (2015).
- ⁴⁸J. Du, C. Catania, and G. C. Bazan, *Chem. Mater.* **26**(1), 686 (2014).
- ⁴⁹V. B. Wang, J. Du, X. Chen, A. W. Thomas, N. D. Kirchofer, L. E. Garner, M. T. Maw, W. H. Poh, J. Hinks, S. Wuertz, S. Kjelleberg, Q. Zhang, J. S. C. Loo, and G. C. Bazan, *Phys. Chem. Chem. Phys.* **15**(16), 5867 (2013).
- ⁵⁰G. T. Charras, B. A. Williams, S. M. Sims, and M. A. Horton, *Biophys. J.* **87**(4), 2870 (2004).
- ⁵¹F. Bianchi, M. Malboubi, J. H. George, A. Jerusalem, M. S. Thompson, and H. Ye, *J. Neurosci. Res.* **97**(7), 744 (2019).
- ⁵²E. S. Haswell, R. Phillips, and D. C. Rees, *Structure* **19**(10), 1356 (2011).
- ⁵³M. R. L. Stone, U. Łapińska, S. Pagliara, M. Masi, J. T. Blanchfield, M. A. Cooper, and M. A. T. Blaskovich, *RSC Chem. Biol.* **1**(5), 395 (2020).
- ⁵⁴J. Cama, M. Voliotis, J. Metz, A. Smith, J. Iannucci, U. F. Keyser, K. Tsaneva-Atanasova, and S. Pagliara, *Lab Chip* **20**(15), 2765 (2020).
- ⁵⁵F. Zhang, L.-P. Wang, M. Brauner, J. F. Liewald, K. Kay, N. Watzke, P. G. Wood, E. Bamberg, G. Nagel, A. Gottschalk, and K. Deisseroth, *Nature* **446**(7136), 633 (2007).
- ⁵⁶M. Jakešová, M. Silverá Ejneby, V. Derek, T. Schmidt, M. Gryszel, J. Brask, R. Schindl, D. T. Simon, M. Berggren, F. Elinder, and E. Daniel Glowacki, *Sci. Adv.* **5**(4), eaav5265 (2019).
- ⁵⁷W. Adam, J. Rivnay, L. Kergoat, A. Jonsson, S. Inal, I. Uguz, M. Ferro, A. Ivanov, T. Arbring Sjöström, D. T. Simon, M. Berggren, G. G. Malliaras, and C. Bernard, *Adv. Mater.* **27**(20), 3138 (2015).
- ⁵⁸J. Delbecke, L. Hoffman, K. Mols, D. Braeken, and D. Prodanov, *Front. Neurosci.* **11**, 663 (2017).
- ⁵⁹I. Tochitsky, J. Trautman, N. Gallerani, J. G. Malis, and R. H. Kramer, *Sci. Rep.* **7**, 45487 (2017).
- ⁶⁰I. Tochitsky, A. Polosukhina, V. E. Degtyar, N. Gallerani, C. M. Smith, A. Friedman, R. N. Van Gelder, D. Trauner, D. Kaufer, and R. H. Kramer, *Neuron* **81**(4), 800 (2014).
- ⁶¹O. K. Nag, M. E. Muroski, D. A. Hastman, B. Almeida, I. L. Medintz, A. L. Huston, and J. B. Delehanty, *ACS Nano* **14**(3), 2659 (2020).
- ⁶²M. G. Shapiro, K. Homma, S. Villarreal, C.-P. Richter, and F. Bezanilla, *Nat. Commun.* **3**(1), 736 (2012).
- ⁶³N. Martino, P. Feyen, M. Porro, C. Bossio, E. Zucchetti, D. Ghezzi, F. Benfenati, G. Lanzani, and M. Rosa Antognazza, *Sci. Rep.* **5**, 8911 (2015).
- ⁶⁴S. Thompson, L. Masukawa, and D. Prince, *J. Neurosci.* **5**(3), 817 (1985).
- ⁶⁵C.-P. Richter, A. I. Matic, J. D. Wells, E. D. Jansen, and J. T. Walsh, *Laser Photonics Rev.* **5**(1), 68 (2011).
- ⁶⁶A. R. Duke, M. W. Jenkins, H. Lu, J. M. McManus, H. J. Chiel, and E. Duco Jansen, *Sci. Rep.* **3**(1), 2600 (2013).
- ⁶⁷C. Paviolo and P. Stoddart, *Nanomaterials* **7**(4), 92 (2017).
- ⁶⁸K. Eom, J. Kim, T. Choi, S. B. Jun, and S. J. Kim, *Small* **10**(19), 3853 (2014).
- ⁶⁹V. Myroshnychenko, J. Rodríguez-Fernández, I. Pastoriza-Santos, A. M. Funston, C. Novo, P. Mulvaney, L. M. Liz-Marzán, and F. J. García de Abajo, *Chem. Soc. Rev.* **37**(9), 1792 (2008).
- ⁷⁰R. Chen, G. Romero, M. G. Christiansen, A. Mohr, and P. Anikeeva, *Science* **347**(6229), 1477 (2015).